



# OPEN Photocatalytic removal of textile wastewater-originated methylene blue and malachite green dyes using spent black tea extract-coated silver nanoparticles

Sikander Ali<sup>1</sup>✉, Huma Ijaz<sup>1</sup>, Muhammad Usman Ahmad<sup>1</sup>, Rukhma<sup>1</sup>, Najeeb Ullah<sup>2</sup>, Abid Sarwar<sup>2</sup>, Muhammad Jalal Khan<sup>3</sup>, Tariq Aziz<sup>3</sup>✉, Ashwag shami<sup>4</sup> & Fahad Al-Asmari<sup>5</sup>

The spent black tea extract was utilized in order to synthesize the spent black tea silver nanoparticles (SBT-AgNPs). Various parameters were tested to yield the best production of SBT-AgNPs. The characterization was conducted by X-Ray diffraction, Scanning electron microscopy, Zeta potential and energy dispersive X-ray (EDX). The XRD analysis showed hkl planes corresponding to (111), (200), (220), (311) planes at  $2\theta$  theta deg 38.3°, 40.8°, 64.5°, and 74.2°. The scanning electron microscopy reported the plate like round shaped morphology of the AgNPs. The zeta potential was examined to be -17.5 mV and a size distribution by intensity of 157.6 d. nm was observed. The EDX was employed to determine the purity of samples by reporting a strong peak of silver (Ag). The degradation activity was examined by photocatalytic removal of methylene blue and malachite green dyes from textile wastewater. The textile wastewater showed a decrease of methylene blue by 25% and 58.3%. The malachite green was also reduced by 33.3% and 60%, which was remarkably significant owing to the presence of the complex factor in the natural environment. The study sets a promising record to harbor the full potential of available food waste resource, such as spent black tea to form SBT-AgNPs and its application in the dye removal from textile waste. The multifaceted outcomes of this study resulted in an eco-friendly procedure, thereby reusing the waste material for environmental cleanup.

**Keywords** Silver nanoparticles, Spent black tea, Methylene Blue, Malachite Green Photocatalytic Degradation

Textile industries are a major source of water pollution where their discharge constitute the large amounts of dyes into the water. Textiles use 100,000 tons of dyes, out of which 10,000 tons of these dyes are discharged in oceans annually. Most of these dyes are carcinogens or mutagenic to human beings<sup>1,2</sup>. These effluents are recognized for their ability to alter the pH of the water, their high oxygen demand, their non-biodegradability, and their resistance to many oxidizing agents<sup>3</sup>. These dyes with complex structures are a great challenge for absolute degradation. Two of these most discharged textile dyes are methylene blue and malachite green<sup>4</sup>. These two textile dyes are responsible for over 20% of dyes based effluent contamination in water. The methylene blue dye ( $C_{16}H_{18}N_3SCl$ , C. I. No. 52015) results in health conditions such as nausea, hemolysis, hypertension, and respiratory diseases. While malachite green ( $C_{23}H_{25}N_2Cl$ , C. I. No. 42000) affects organs like the eyes, kidneys, liver, and bones, reduces food intake, and targets respiratory enzymes in fish population<sup>5</sup>. The traditional biological treatment methods have been proved to be futile with these dyes resistant to well-known biological

<sup>1</sup>Department of Microbiology, Dr. Ikram-ul-Haq Institute of Biotechnology, Government College University Lahore, Lahore, Pakistan. <sup>2</sup>Food and Biotechnology Research Center, PCSIR Labs Complex Lahore, Lahore, Pakistan. <sup>3</sup>Beijing Advanced innovation Center for Food Nutrition and Human Health, Beijing Technology and Business, University, Beijing, China. <sup>4</sup>Department of Biology, College of Science, Princess Nourah bint Abdulrahman University, Riyadh 11671, Saudi Arabia. <sup>5</sup>Department of Food and Nutrition Sciences, College of Agricultural and Food Sciences, King Faisal University, Al Ahsa 31982, Saudi Arabia. ✉email: dr.sikanderali@gcu.edu.pk; iwocdkd@gmail.com; iwocdkd@gmail.com

agent e.g. microorganisms. Likewise, the chemical and physical treatments are unsuccessful for dyes present in higher concentrations<sup>6</sup>.

Presently, the field of nanotechnology has been explored vastly for the solutions of complex problems, such as wastewater treatment using silver nanoparticles. The interest in silver nanoparticles (AgNPs) for biodegradation and bioremediation has evolved immensely due to their greater surface area to volume ratio and higher reactivity<sup>7–9</sup>. The AgNPs can be produced by various methods such as chemical, photochemical, electrochemical, microwave<sup>10</sup> and sonochemical synthesis<sup>11,12</sup>. However, the green synthesis of AgNPs offers several advantages including environmental sustainability, cost efficiency, biocompatibility, and high product yield, along with superior biological characteristics relative to conventional chemical and physical processes<sup>13–15</sup>. The benefits also include easy scalability on a large scale, no high pressure or temperature, harmful chemicals and energy, and no toxic byproducts<sup>16</sup>. Thus, the method known as green synthesis is a favorable alternative to other fabrication techniques, because of its reliance on eco-friendly substitutes to degrade textile dyes is in high demand<sup>17–19</sup>.

Numerous biological sources, such as microorganisms and their enzymes, plants and their extracts, and other organic wastes have been utilized for the synthesis of AgNPs<sup>16</sup>. However, plant resources (including leaf, peel, bark fruit, root and seed extracts) contain numerous bioactive compounds such as, flavonoids, polyphenols, saponins, proteins, or sugar, as reducing and capping agents for nanoparticles synthesis<sup>20,21</sup>. Among these plant sources, spent black tea, a readily available agro-waste, is considered as a rich source of bioactive phenolic compounds, alkaloids and antioxidants<sup>22–24</sup>. The hydroxyl groups in tea polyphenols donate electrons and reduce silver ions to metallic silver through redox reaction<sup>25</sup>. The aromatic ring and hydroxyl groups in the polyphenols form a protective capping layer around NPs via H-bonding and van der Waals forces to prevent agglomeration. The other organic compounds found in spent black tea (SBT) are the caffeine, tannic acid and polysaccharides, which stabilize the reaction mixture containing AgNPs and prevent the formation of silver agglomerates without the need for additional chemical reagents<sup>16,26</sup>. That's why, SBT-AgNPs exhibit superior stability over various other waste materials, including green tea and coffee, to produce nanoparticles.

It is a well-known fact that black tea is one of the most consumed drinks worldwide especially in South Asia. According to Pakistan Bureau of Statistics Report (2017), every Pakistani consume 15 kg of black tea annually and after consumption, spent black tea is discarded as a biowaste. Thus, the effective and reasonable usage of the spent tea is very crucial<sup>18</sup>. This biowaste is an efficient, cost-effective and scalable medium for the synthesis of SBT-AgNPs under milder reaction conditions<sup>21,23</sup>, due to its abundance as agricultural waste, which ensures low-cost production of AgNPs, its high polyphenolic content, which facilitates efficient reduction and stabilization of AgNPs, and its simple preparation procedure, making it easier to scale compared to other biological methods that require complex cultivation and processing techniques. The prepared SBT-AgNPs work as a redox catalyst for dye degradation by exerting electron relay effect on the donor and acceptor molecules, thereby enhancing the breakdown of dyes<sup>27</sup>. Paired with the photocatalysis, a method wherein the excited electrons of a valence shell to conduction band upon sunlight irradiation, cause electron-hole pair generation. The resulted OH<sup>•</sup> radical acts as a strong oxidizing agent and completely degrades the dye to non-toxic products such as, CO<sub>2</sub>, H<sub>2</sub>O. Thus, this study was conducted with the aim of degradation of methylene blue (MB) and malachite green (MG) in the absence and presence of sunlight to determine the potential of SBT-AgNPs<sup>28,29</sup>.

The multifaceted objective of this research was to practically understand the degradation nature of actual dyes methylene blue and malachite green released in textile waste rather than lab prepared solutions. Besides, the study aimed to utilize only free or very cost effective spent or waste raw material which no one wanted, to step one foot ahead toward the convenience and practicality in green chemistry. As per our knowledge, it is only study which has used spent black tea to synthesize the AgNPs as well as studies dyes in textile waste with prominent outcomes.

## Materials and methods

The analytical grade chemicals such as, silver nitrate (ACS Grade, ≥ 99.0%) and trisodium citrate (ACS Grade, ≥ 99.0%) were procured from Sigma-Aldrich (Germany). The wastewater was collected from Nishat Chunian textile plant, Lahore.

### Synthesis of spent black tea extract

The spent black tea extract was formed by adding 0.5 g of spent black tea powder in 8 ml of distilled water. The mixture was heated for 2 min in microwave oven at H mode. The mixture after heating was brought to room temperature, filtered and supernatant was collected. The supernatant was freeze at -20 °C for 120 h and later was stored at -4 °C for better stability.

### Synthesis of SBT-AgNPs

The experiment to biosynthesized AgNPs was conducted by using method previously described by Qing *et al*<sup>18</sup> in his study on AgNPs formation from waste tea extract. The spent black tea AgNPs were synthesized by adding 1 ml of spent black tea extracts in 9 ml of (100 mM) AgNO<sub>3</sub> salt. The solution was kept at 70 °C and 120 rpm for 1 h. After reaction was achieved, the mixture was adjusted to surrounding temperature and centrifuged for 20 min at 6000 rpm. The pellet was collected and rinsed with distilled water three times and centrifuged alternatively. The ultimate pellet was dissolved by introducing 3 ml of distilled water in the falcon tube. It was characterized by UV-VIS spectrometer. For the analysis, the sample (3 ml) was poured into a quartz cuvette, and the wavelength was set from 200 to 800 nm. The data was recorded. By using data from the analysis, spectra depicting the activity as peaks were plotted in the origin software<sup>30</sup>.

### Optimization of parameters for AgNPs synthesis

Various reaction parameters such as  $\text{AgNO}_3$  concentration, SBT extract concentration and reaction time were optimized by one-factor-at-a-time (OFAT) method. 1 ml of varying concentration (1, 10, 50 and 100 mM) of  $\text{AgNO}_3$  salt was added to the 9 ml of the prepared extract. Furthermore, the varying concentration (1, 2, 3 and 4 ml) of extract was optimized by using the previously optimized salt concentration. The reaction time (30, 60, 90 and 120 min) of AgNPs biosynthesis was studied. The hot water bath was set at 70 °C and 120 rpm for the maximum bioactive compound's extractions. Furthermore, the reaction mixture was allowed to cool down at room temperature and centrifuged for 20 min at 6000 rpm. After centrifugation, the pellet was rinsed thrice with distilled water and dissolved. The progress of the process was also monitored by UV- VIS spectroscopy.

### Chemical synthesis of AgNPs

The chemically synthesis of silver nanoparticles was conducted by method described by Ahari et al.<sup>31</sup> with some adjustments. The chemically synthesized AgNPs were produced by using tri-sodium citrate ( $\text{Na}_3\text{C}_6\text{H}_5\text{O}_7$ ) as reducing agent. The 10 ml of  $\text{AgNO}_3$  salt (50 mM) solution was placed in a water bath for 1 h at 80 °C and then the  $\text{Na}_3\text{C}_6\text{H}_5\text{O}_7$  solution was added drop by drop until a color transition was observed (from milky white to yellowish brown). Periodically, the flask was shaken for the sake of the effective mixing of the reactants. After the reaction had been completed, the temperature of the mixture was let to adjust with that of surrounding environment of room and centrifuged eventually at 6000 rpm for 20 min. The pellet obtained was subject to washing with distilled water. The eventual pellet was liquefied by adding distilled water (3 ml) and characterized by UV-VIS spectroscopy.

### Characterization of AgNPs

The AgNPs were characterized by the various techniques such as UV-Vis spectroscopy, X-ray diffraction (XRD) analysis, scanning electron microscopy (SEM), and zeta potential.

### UV-VIS spectroscopy

The whole experiment was monitored by UV-VIS spectroscopy during synthesis and in optimization<sup>32</sup>. The UV-VIS spectroscopy was also a core technique to study dye degradation. The liquid samples were analyzed in the wavelength range of 200–800 nm via UV-Vis spectrophotometer<sup>26</sup>. The optical density (OD) was used as output from the calculation of unhindered light subtracted from the total light. The OD was recorded as absorption signal against wavelength.

### X-Ray diffraction analysis (XRD)

The XRD was utilized to study the particles size, dimensions and crystalline nature. The sample was prepared in dense liquid form. The XRD instrument (D8 discover, Bruker) which was used for the analysis operated with scan speed 1 in the  $2\theta$  range from 5° to 80° and examined about the crystalline nature of the SBT-AgNPs. The gadget produced  $\text{K}\alpha$  of wavelength 0.15406 nm by utilizing copper anode<sup>33</sup>. The sample holder carried the sample while the X-ray passes over it. The beam of the X-rays stroked the sample and bent due to diversion by the atoms of the crystal lattice in the sample. The resulting diversion of beam was recorded for XRD results as a signal.

### Scanning electron microscopy (SEM)

The scanning electron microscopy was conducted to elaborate on the size distribution and estimation of the morphology of SBT-AgNPs. A sample of the SBT-AgNPs were prepared in the powdered form by oven drying method and headed to Syed Babar Ali School of Science and Engineering, Lahore University of Management Sciences (LUMS), Lahore. The sample was put into the SEM chamber specified for the sample. The relevant stage was adjusted in order to get diverse angles of images. A focused beam of electrons stroked the sample and released multiples signals specifying the position and shape of AgNPs. The scanning electron microscope analyzed those signals to generate an image of the surface of the particles.

### Zeta potential measurement and EDX

The powdered SBT-AgNPs sample was dispatched to the Lahore University of Management Sciences (LUMS), Lahore for zeta potential and EDX analysis from Syed Babar Ali School of Science and Engineering. Before analysis, the sample was sonicated and then examined by nano ZS instruments (Malvern Instruments Ltd, Zeta sizer Ver. 7.10) for zeta sizing. The examination was carried out per count rate of 253.3 kcps in the zeta potential range of -150 mV to 150 mV at room temperature. This analysis depicted the SBT-AgNPs stability. The adjustment was made to measurement position at 2 mm.

### Applications coated-AgNPs for the removal of dyes

The cation dyes methylene blue and malachite green present in textile wastewater were used to test the dye degradation capabilities of biosynthesized SBT-AgNPs.

### Preparation of standard dye of methylene blue and malachite green

The methylene blue degradation was studied by a method described in Trieu et al.<sup>29</sup> work with some amendments. The standard solution of methylene blue was prepared to examine the peaks pattern of these dyes to detect the peaks of dyes present in textile waste. The powder methylene blue was retrieved from chemical store in IIB. The varying concentrations of dyes (0.05 ,0.1 ,0.15 ,0.2 ,0.25 and 0.3 mg) were prepared from stock solution of 30 mg/L and dissolved in 10 ml of sterile distilled water. Their absorption was measured in UV/Visible spectroscopy at range of 200–800 nm. The malachite green degradation was studied under the guidance of

method suggested by Iqra et al.<sup>34</sup>. The varying concentrations of malachite green (100, 200, 300, 400, 500 mg) were prepared from stock solution of 1 g/L. The UV/Vis spectroscopy was conducted on the standard solution of dye to plot spectra in origin software.

### Degradation of standard dyes

Similar to the above procedure, two test tubes of 9 ml of standard dye of methylene blue (0.05 mg/ml) was prepared and 1 ml of SBT-AgNPs was added to each of the test tube. One of was then exposed to room light and other was kept in sunlight for 180 min. Another solution with same concentration and without AgNPs was prepared to compare with AgNPs solution. For malachite green degradation studies, two test tubes of 9 ml of malachite green (0.1 mg/ml) was prepared and 1 ml of SBT-AgNPs were added in each test tubes. The one of reaction mixture was then let to stay in condense light and other under sunlight for 180 min. After the experiment, all these three solutions were analyzed by UV/Vis spectroscopy.

### Preparation of textiles dye waste

The concentrations of dyes (1 µl) were prepared and analyzed in UV-Vis spectroscopy and their spectra were constructed in the origin software.

### Dye degradation of the textile waste

In 2 test tubes, 9 ml of (0.001 mg/ml) concentration of textile wastewater was taken. The biosynthesized SBT-AgNPs (1 ml) were added to both solutions. One was kept under a room light and the other was put in sunlight for 180 min. A test tube with a freshly prepared textile wastewater solution with same concentration as prior solutions, however, without SBT-AgNPs was prepared to compare the extent of degradation of dyes by AgNPs. After reaction time has passed, these three solutions were examined by UV/Visible spectroscopy.

## Result and discussion

### Preparation of extract

The extract of spent black tea in UV-Vis gave a peak when the biomolecules in the extract absorbed the passing rays. The higher the density of absorption, the richer the extract was concluded<sup>35</sup>. The UV-Vis analysis showed that the biomolecules in the extracts (prepared with 0.5 g of spent black tea in 8 ml of distilled water heated for 120 s at H mode) showed a characteristic peak at 350 nm at absorption signal of 2.29 (Fig. 1).

### Green formation of spent black tea silver nanoparticles (SBT-AgNPs)

#### *Optimization of salt concentration for SBT-AgNPs*

The AgNPs were prepared by varying the concentration of salt (1, 10, 50, 100 mM) in spent black tea<sup>36</sup>. The presence of a dome-shaped broad peak at 423 nm corroborated the presence of the formed nanoparticles. In the peaks of Fig. 2, the peaks associated with the 100mM showed highest absorption signal of 2.8. This peak also showed maximum jerks in the dome. The peaks associated with the 50mM peak exhibited a more normal dome at the 2.35 OD. Moreover, peaks associated with the 1 and 10 mM AgNO<sub>3</sub> showed less distinctive peaks. However, the dome associated with the 10 mM salt was more defined as compare to the 1 mM concentration<sup>37</sup>. The efficient synthesis was considered from the 50 mM AgNO<sub>3</sub> which gave comparatively more absorption signals compared to 100mM salt concentration only making a difference of 0.45 OD points. The study by Nikam & Chaudhari<sup>38</sup> seconded the result that increase in the concentration of salt increased the yield of AgNPs. Further increased in the concentration after 50 mM resulted in jerks and noise in the spectra. It was observed that the peak correlated to 50 mM was a little narrower than 100 mM which suggest better size distribution. Furthermore, the peak correlated to 50 mM showed at 417 nm while the peak correlating to 100 mM redshifted to 423 nm, implying that particle size has increase. The peaks are a perfect dome shaped with the same high points at same wavelength of 423 nm<sup>37</sup>. Thus, the peaks associated with 50mM was considered ideal concentration of salt (Htwe et al., 2019). The dome-shaped peaks in the UV-Vis spectra are indicative of green-synthesized AgNPs. The peak at 423 nm indicates the formation of black tea AgNPs. The peak height represents the intensity of AgNPs, whilst the breadth shows the range of AgNPs sizes present in the reaction mixture.

#### *Optimization of biomass volume for synthesis of SBT-AgNPs*

The optimization of the salt concentration followed the optimization of biomass extract volumes for effective synthesis of the SBT-AgNPs<sup>37</sup>. Consequently, SBT-AgNPs were prepared by biomass to salt ratios of 1:9, 2:8, 3:7 and 4:6. In the spectra Fig. 3, the peak associated with 2 ml of biomass in 8 ml of 50 mM AgNO<sub>3</sub> salt showed most dominant peak at 2.2 absorption signal. Followed this peak was the peaks linked with 3:7 and 1:9 ml biomass volume. The biomass volume of 4 ml showed the most disruptive dome with sharper many peaks and junk. It can probably be associated with the formation of some biproducts which too required an optimum biomass to salt ratio. The result from the level of biomass suggested that up to biomass level (2 ml), AgNPs synthesis peaked owing to the high level of reducing agent available for the synthesis and capping of the AgNPs<sup>38</sup>. However, after this level, the increase in biomass plunged the SBT-AgNPs synthesis owing to decrease in the Ag<sup>+</sup> ions availability. Furthermore, the higher concentration of biomass led to higher formation of agglomerate forming compound and sugars present in spent black tea leading to junks and noise at higher concentrations<sup>39,40</sup>.

#### *The optimization of reaction time for the synthesis of SBT-AgNPs*

The spectra leading to the optimization of reaction time was studied over the time periods of 30 to 120 min<sup>41</sup>. The spectra precisely described the effect of reaction time on the green synthesis of SBT-AgNPs. The Fig. 3 associated with the SBT-AgNPs exhibited dome shaped peaks at 425 nm with the peaks associated with time period of 30, 60 and 90 min suitable for study while the peak linked with 120 min was abandoned owed to

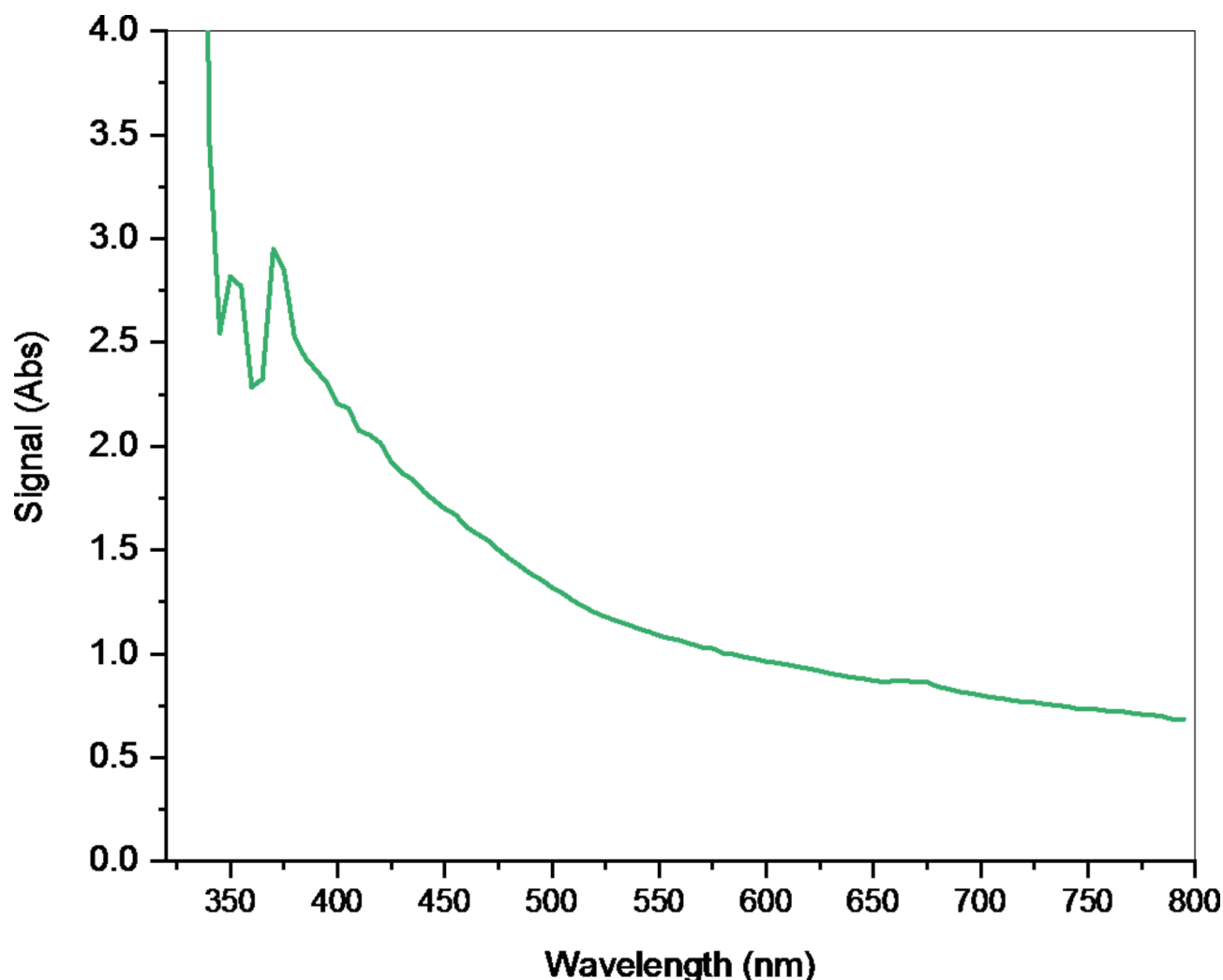


**Fig. 1.** SPR resonating spent black tea extract.

disruptions in its dome. The peak linked with 90 min has an absorption density of 2.9 while the peak of 60 min has ascent rise of 2.6. The ascent of 60 min peak showed a clear mark of 1.2 as compared to the peak associated with 30 min time. The mark was a significantly reduced from 60 min peak to 90 min peak. Thus, it can be safely assumed that 60 min time was more efficient than the 90 min reaction time in spent black tea mediated synthesis of AgNPs. Al-Hashmi<sup>42</sup> also described that 90 min should be the maximum heating time to green synthesize the AgNPs on his study of spent coffee mediated AgNPs.

Finally, the optimized SBT-AgNPs were synthesized by 2 ml of spent black tea biomass in 8 ml of 50 mM of  $\text{AgNO}_3$  salt and heated for 60 min in the water bath at 70 °C (Fig. 4a). The increase in time suggested the increase in contact time for Ag ions and the spent black tea extract reducing agents<sup>43</sup>. However, after 120 min the enhance contact time showed the noise and junk in the peaks corresponding to the 90 and 120 min. this could also lead to the agglomeration of AgNPs by sugar and other preserving compounds present in the spent black tea. The chemically synthesized AgNPs also showed their characteristic peak at 310 nm. In the following characterization the SBT-AgNPs and these chemically synthesized AgNPs will be compared against each other for their particles size, shape, and stability (Fig. 4b).

## Characterization studies

### X-Ray diffraction analysis

The XRD analysis was conducted on the samples of SBT-AgNPs and chemically synthesized AgNPs to reveal their crystalline nature. The X-Ray diffraction on samples reveals the crystal structure, phase composition and structural changes<sup>44</sup>. The scan speed was kept at 1 s per step. The angle 2 theta was ranged from 0 to 80°. The tool consisted of a copper anode and monitored at  $\lambda$  wavelength of 0.15406 nm. Figure 5a and b demonstrated the XRD profile of SBT-AgNPs and chemically synthesized AgNPs. The peaks corresponding to SBT AgNPs 2 $\theta$  were found to be at 38.3°, 40.8°, 64.5°, 74.2°. The hkl planes at (111), (200), (220), and (311). The peaks representing the chemically synthesized AgNPs appeared at 38.1°, 44.3°, 64.4°, 81.5°. The hkl planes relating to respective peaks were determined to (111), (200), (220), and (311) according to the data from Ref: Joint



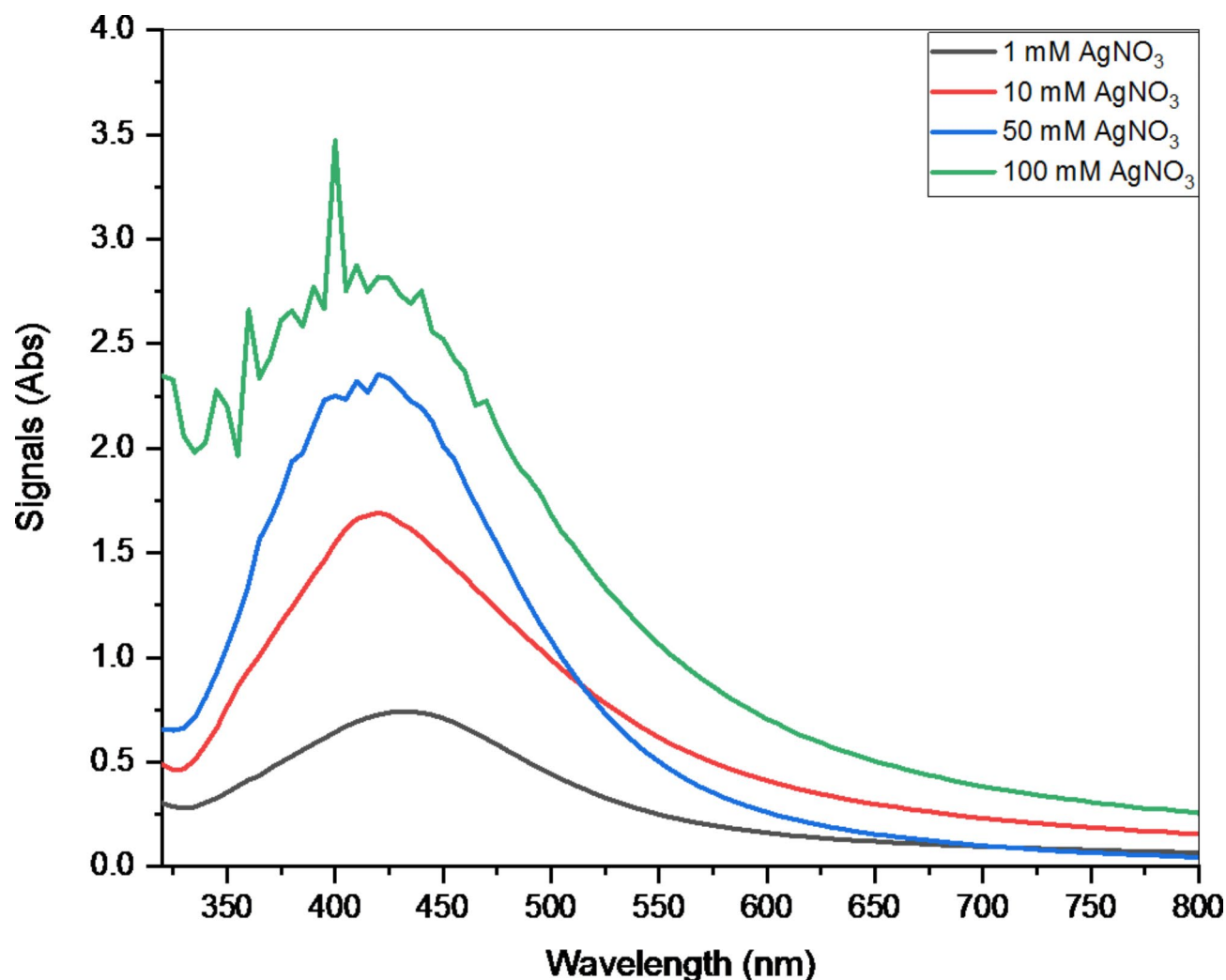


**Fig. 2.** The absorption spectra depicting the effect of salt concentration on the production of SBT-AgNPs synthesis by using spent black tea extract.

Committee on Powder Diffraction Standards, JCPDS file No. 04-0783. The most intense peak correlates to the polycrystalline phase composition of formed AgNPs corroborating the formation of face-centered cubic (FCC) crystalline AgNPs. The output from the XRD analysis affirmed that the AgNPs formed were FCC crystalline structure nanoparticles, in which the (111) hkl peak is the most dominant and it possessed a surface with an atomic arrangement<sup>45</sup>. Similar results has been suggested by Manikandan et al.<sup>46</sup> in their study for production of AgNPs using the *Ocimum Americanum* or Hoary Basil leaf extract and the hkl planes (111), (200), (220), and (311) corresponding to the successful formation of AgNPs were reported. It was also found that the long reaction time also supported the strong crystalline structure of AgNPs. Li et al.<sup>47</sup> studied the effect of reaction time on crystalline phase and indicated that an increase in reaction time led to formation of single crystalline form as compared to polycrystalline structure formed during early reaction time.

In another study, Ninsiima et al.<sup>48</sup> used the green method of formation of AgNPs. The XRD analysis was carried out for determining the crystalline nature of silver nanoparticles. The peaks corresponding to (111), (200), (220), and (311) planes were found successfully indicating the face centered cubic structure of silver nanoparticles. The angles and their hkl planes determined in our study also co-related with those of Shyamalagowri et al.<sup>49</sup> on their study of AgNPs production from *Hylocereus undatus* extract. The angles corresponding to planes at (111), (200), (220), and (311) were found, which resonated the formation of face centered cubic AgNPs. Hence the SBT-AgNPs were classified as the face centered cubic (FCC) AgNPs.

### Scanning electron microscopy

SEM was performed to get the images of SBT-AgNPs at higher resolutions in order to analyze the morphology of AgNPs. SEM was utilized for examining the size of SBT-AgNPs (Sadeghi and Gholamhoseinpoor, 2015). SEM images were illustrated at 7000 X, 25,000 X, 50,000 X and 100,000 X (Fig. 6). In term of morphology, the images showed that the SBT-AgNPs at lower resolution appeared to have a coral-like shape. The high-resolution SEM images exhibited that the individual SBT-AgNPs were plates shaped and chemically synthesized AgNPs

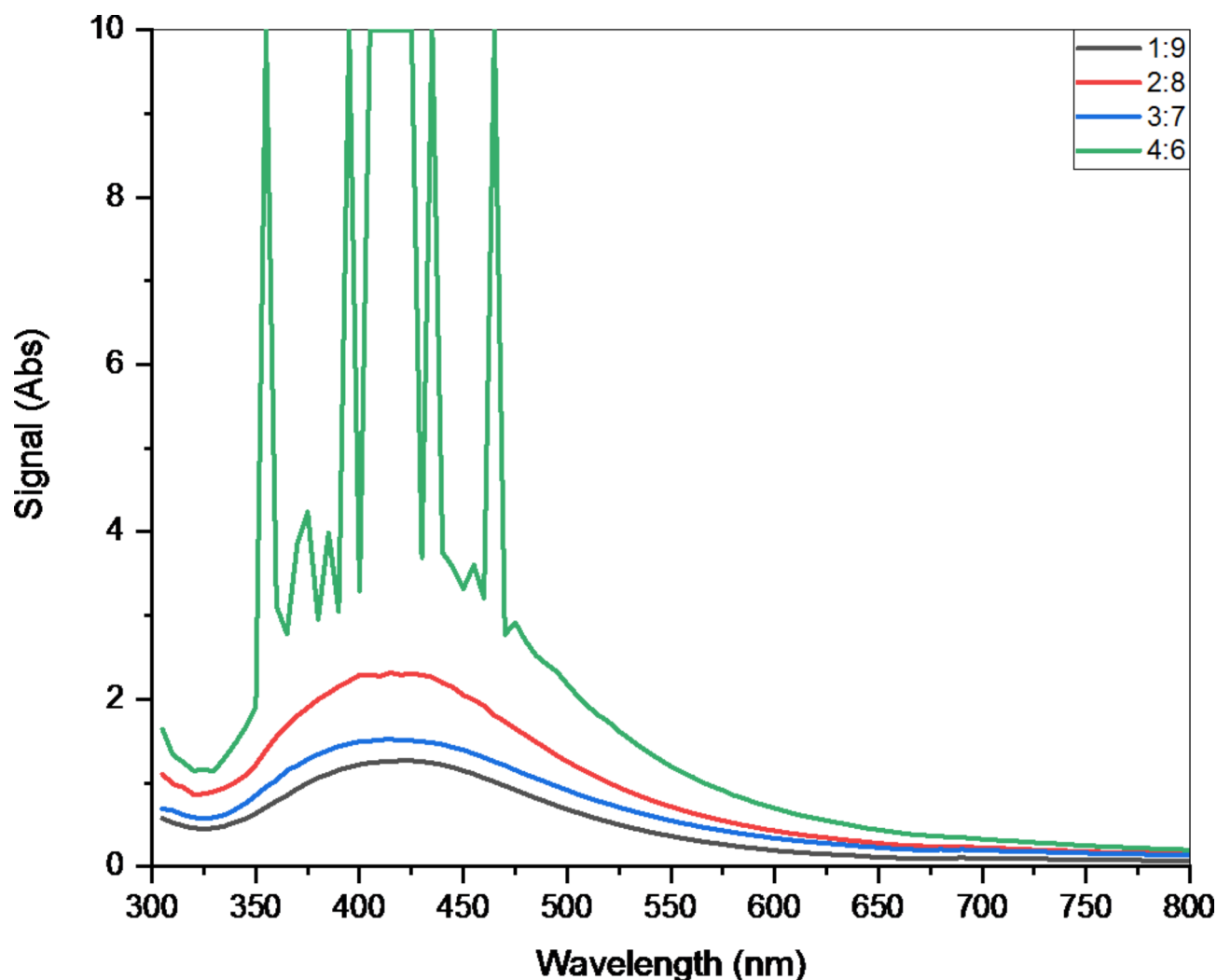


**Fig. 3.** The absorption spectra of SBT-AgNPs depicting the effect of salt to spent black tea biomass ratio on AgNPs formation.

were porous shaped particles. The chemically synthesized AgNPs appeared to be like interwoven channels, with nanorods or nanoflakes shapes. The SBT-AgNPs were mostly placed separately, however, the chemically prepared AgNPs were in aggregates. Goyal et al.<sup>51</sup> observed the smaller (~43 nm) triangular and hexagonal nanoparticles with rounded corners. The overall shape of the SBT-AgNPs were mushy and fibrous in appearance at lower resolutions. The chemically prepared AgNPs appeared as interwoven networks at lower magnification, indicating the aggregates formation. Plate-like and well-dispersed SBT-AgNPs have a higher surface area and better accessibility to catalytic sites, thus increasing their efficacy in dye degradation compared to chemically synthesized AgNPs. The image J software was used to find the particle size of AgNPs<sup>50</sup>. The image J software predicts the average particles size of SBT-AgNPs to be 99.3 nm. While the minimum particle size was calculated to be 6 nm and largest particles size was identified to be 225 nm. The chemically synthesized AgNPs has the particles size of average particle size of 114 nm. The minimum particle size was found to be 24 nm and maximum particle size was recorded to be 179 nm. Overall, the particle size of SBT-AgNPs were finer than chemically synthesized AgNPs.

The little contact of the AgNPs with each other in the SBT-AgNPs has been describe by Parvathalu et al.<sup>50</sup> owing to the owing to good capping and stabilizing effect of spent black tea extract. The presence of clear zone indicates the inhibition of bacterial growth by nanoparticles. However, this inhibition is considerably different for nanoparticles of different shapes. Although, all the samples were plate-like nanoparticles, but they differ in their size and edges and hence show different antibacterial activity against both Gram-positive and Gram-negative bacteria<sup>51</sup>.

### Zeta potential

Zeta potential analysis is done to estimate the stability of AgNPs. Zeta potential provided the information about stability and surface charge of colloidal SBT-AgNPs<sup>18</sup>. The system was set at 25 °C for 12 zeta runs. The designed count rate was 253.3 kcps. However, measurement position was 2 mm. In this study, the observed zeta potential

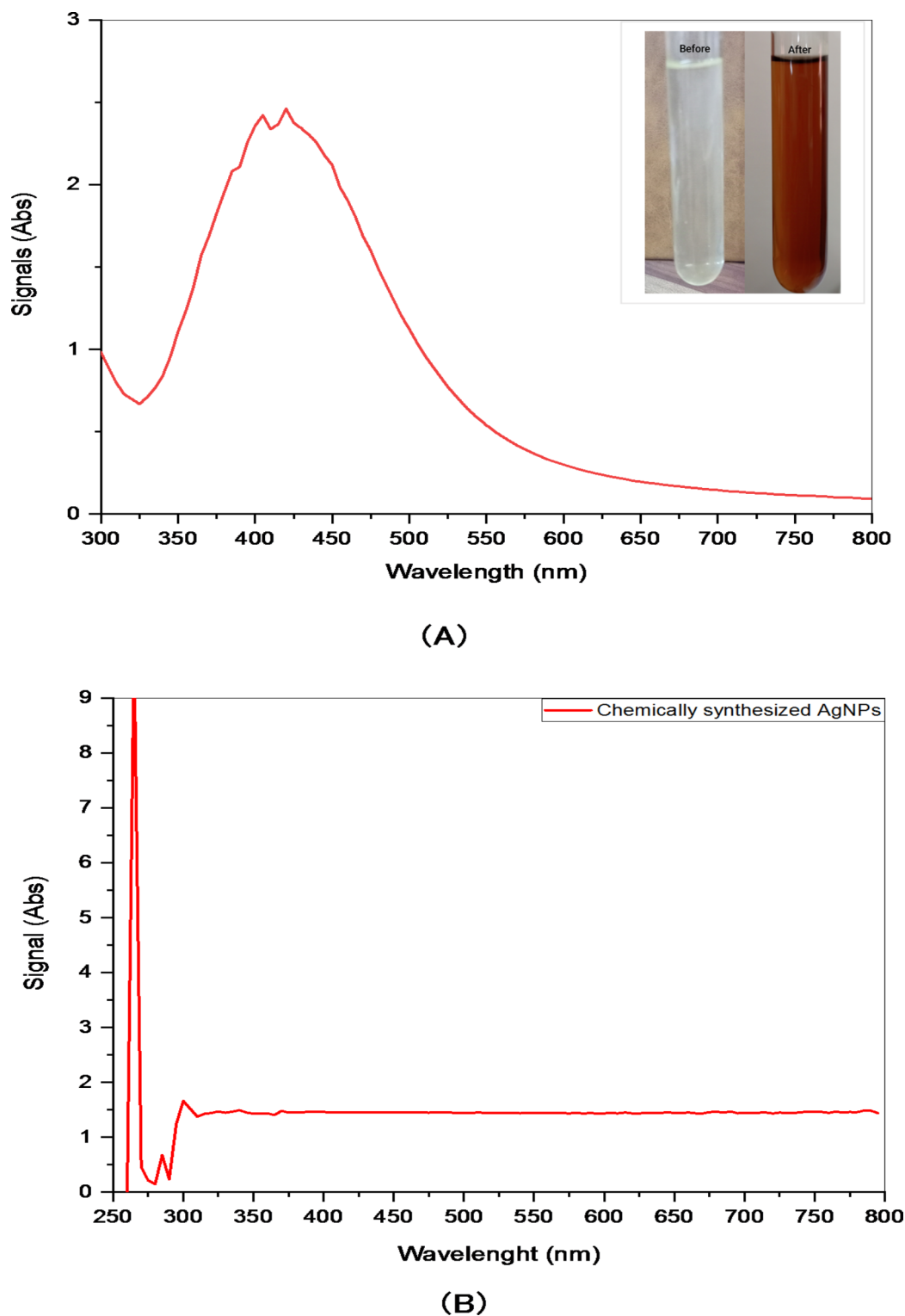


**Fig. 4.** The final absorption spectra of (a) SBT-AgNPs and (b) chemically synthesized AgNPs.

was  $-13.6$  mV for chemically synthesized AgNPs (Fig. 7b) and SBT-AgNPs (Fig. 7a) were observed to be  $-17.5$  mV with zeta deviation of 10.8 and  $-13.7$  mV indicating the stability of silver nanoparticle suspension. The occurrence of a sharp peak at  $-13.6$  and  $-17.5$  mV indicated that AgNPs are negatively charged and dispersed in the medium. Our results were found to be perfectly consistent with the results of Qing et al.<sup>18</sup>, which showed moderate colloidal stability due to high electrostatic repulsion, thus preventing the agglomeration between particles. Furthermore, the appearance of negative charge has been resulted to prevent the aggregates formation. Qing et al.<sup>18</sup> justified the negative potential value could be due to the presence of bioorganic components in the



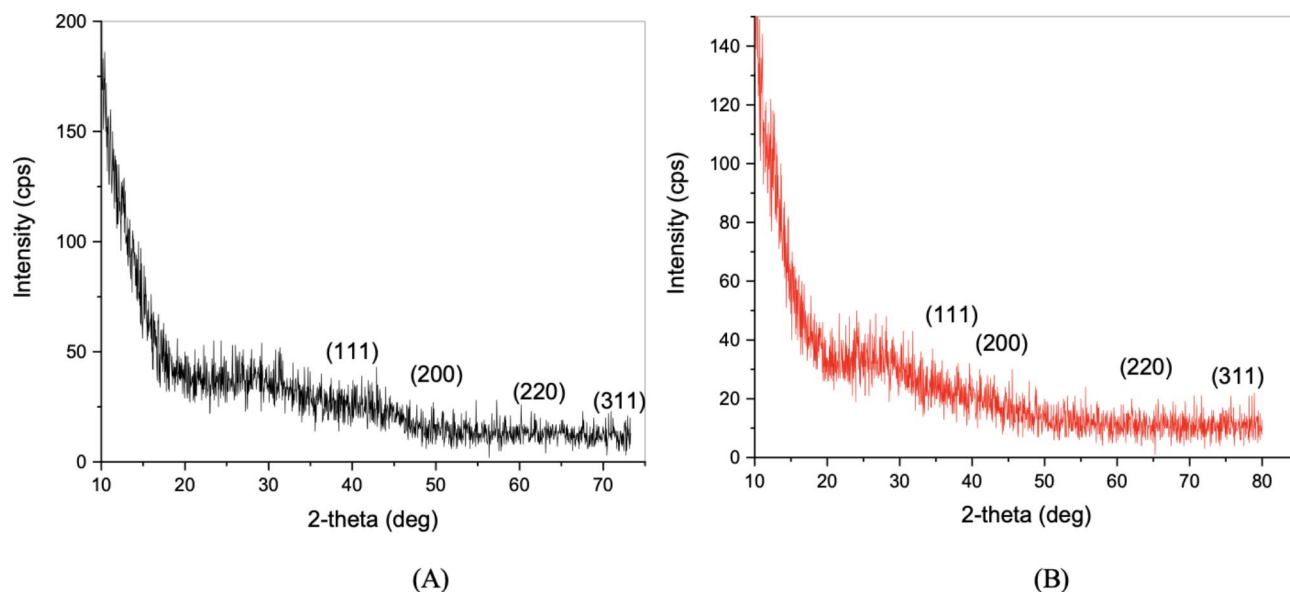


**Fig. 5.** XRD analysis of SBT-AgNPs (A) Chemically synthesized AgNPs (B).

extract as capping agent. Giri et al.<sup>52</sup> described that the negative charges represent the repulsion between the particles to prevent aggregate formation, thus indicating the stable nature of AgNPs. The results of this research about SBT-AgNPs subside with the studies indicating the AgNPs are well dispersed and stable.

Al-Ogaidi et al.<sup>22</sup> explained that the long-term stability of the tea-extract synthesized colloidal AgNPs was monitored through the zeta potential which was used to establish the properties of the surface of the AgNPs. The predominance of either positive or negative surface charges in nanoparticles has been generally claimed as necessary for the stability of colloidal inorganic nanoparticles. The inorganic nanoparticles with a large positive or negative zeta potential had been shown to repel each other, thereby, preventing aggregation. It has been reported that low absolute zeta potential values lead to aggregation and flocculation due to the absence of repulsive force (Cataldo, 2014). Thus, the zeta potential SBT-AgNPs of -17.5 mv was found to repel each other and prevent aggregates ensuring long term stability.

### Energy-dispersive xray

The energy-dispersive X-ray technique is an identification technique which excite electrons in the sample to release characteristics X-ray. The analysis of EDX spectrum of SBT-AgNPs exhibited various signals relating to the presence of elements such as Ag, Cl, C, O, and S. The signal corresponding to the Ag element showed a sharper presence, while weak signals of other elements were observed. These signals represent the other compounds such as polyphenols, flavonoids, tanins, catchins, glycosides, proteins and saponins present in the extracts (Fig. 8). The EDX studies were corroborated by the previous works<sup>50</sup>.

### Dye removal from textile effluents using immobilized AgNPs

The textile dyes are long persisting, non degradable dyes that not only hinder the visibility for the species living in the water body where they are disposed, but also toxic and threaten the life of the organisms as well as pollute air<sup>53</sup>. The cross contamination with the ground water can risk the human health. This study first detected the presence of dyes in the collected textile waste water and then successful degradation of these dyes. The standard dyes of methylene blue and malachite green were prepared in the lab and were analyzed by UV/Vis spectrometer<sup>54</sup>. The resulting spectra were constructed in the origin95 software. A concentration of the textile waste was prepared to compare all the spectra to detect presence of these dyes (Fig. 9a) The standard spectra of methylene blue was prepared by analyzing the 6 concentrations (0.05, 1, 1.5, 2, 2.5, 3 mg) in 10 ml of distilled water. When examined at the range of 300–800 nm, the dye showed an absorption peak at 665 nm with a shoulder at 610 nm. The peaks were perfectly distanced equally corresponding to the difference between the lowest and highest concentrations. The peak maxima was observed at 0.51 and lowest peak was exhibited at 0.125 nm. The peak rise was dependent on the concentration of the dye (Fig. 9b). The standard spectra of malachite green was constructed by using data from 5 concentrations of (100, 200, 300, 400, 500 mg) dye solution prepared in 10 ml of distilled water. The spectra exhibited the peak maxima at 614 nm. The spectrum also witnessed the accompanying smaller peak at 430 nm. Rise of peak depended on the concentration of the dye in water. The peak maxima corresponding to 500 mg of dye reached to 2.5 optical density (Fig. 9c).<sup>55</sup>

After preparation of the standard dyes, the textile waste spectrum was prepared to relate with the standard to detect dyes by observing peaks at the specific wavelength. Due to high Viscosity of the textile waste a successful spectrum with 1 µl/ ml dye was prepared. The resulting spectra showed 4 peaks at 390, 410, 614 nm. The spectra also give a hump like raise at the 665 nm. The peaks at 614 and 665 nm signaled the presence of malachite green and methylene blue respectively. Although concentration of maachite green was highest in the textile waste water

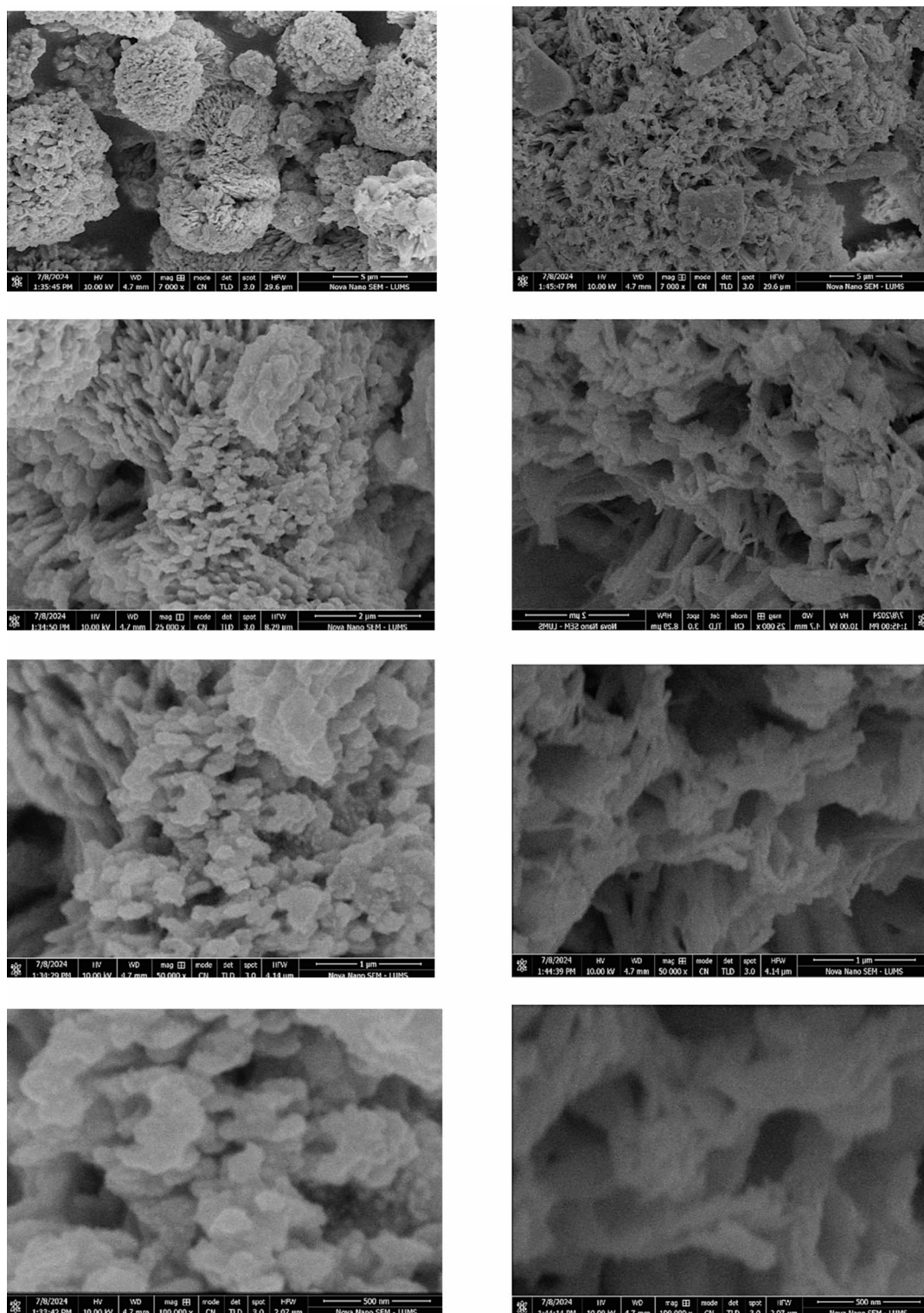


**Fig. 6.** The scanning electron image of SBT-AgNPs (left) and chemically synthesized AgNPs (right) at 7,000X, 25,000X, 50,000X and 100,000X resolutions.

mixture, the water also contained a small amount of methylene blue (Fig. 10). Succeeding the detection of the dyes, the degradation of the dyes was studied. the two test tubes of each sample (0.05 mg/ml of methylene blue, 100 mg/ml of malachite green and 1  $\mu$ l/ml of textile waste) was prepared with 1 ml of SBT-AgNPs. One testube was placed in the condensinging light. other sample were kept in sunlight near window. The resulting spectras were helpful to detect dyes, however it did not reflected on the concentration present of each dye in the waste. thus one fresh test tube without the SBT-AgNPs of each sample without exposing to sunlight was analysed in the

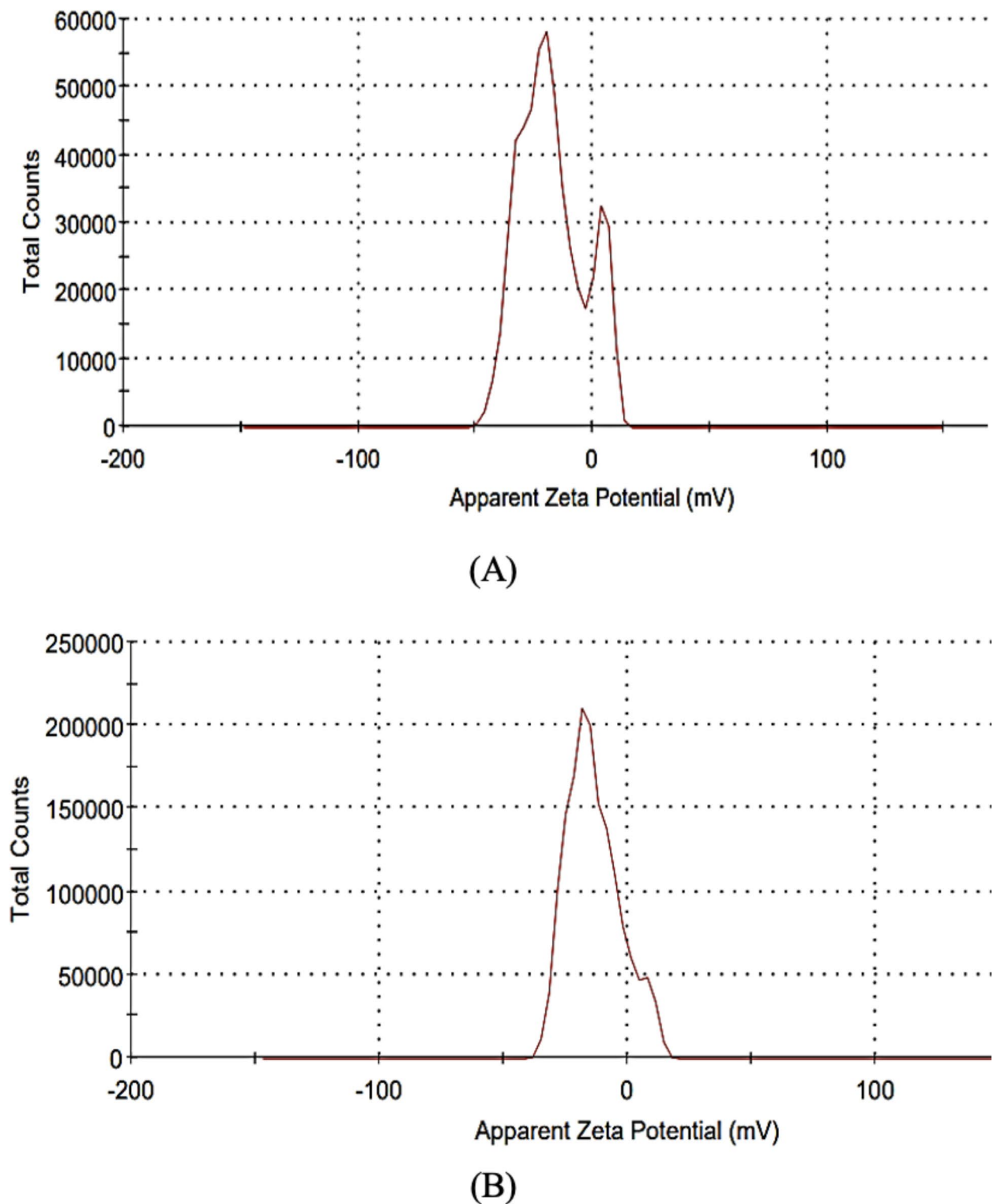


**Fig. 7.** Zeta potential distribution of SBT-AgNPs (A) and chemically synthesized AgNPs (B).

UV/Vis spectrometer and recorded as absorption signal at initial concentration<sup>56</sup>. The absorption signal of final concentrations of both kind of samples (condensing and sunlight) were recorded after 180 min. Resultingly, the spectra with the degradation percentage aided in the studying efficiency of the SBT-AgNPs. the results were substantiated by other related studies such as Trieu et al.<sup>29</sup> showed effectively showed the harmonious impact of sunlight and AgNPs on the methylene degradation. Iqra et al.<sup>34</sup> presented a detailed study on role of capping agents such as green tea for the degradation of malchite green.

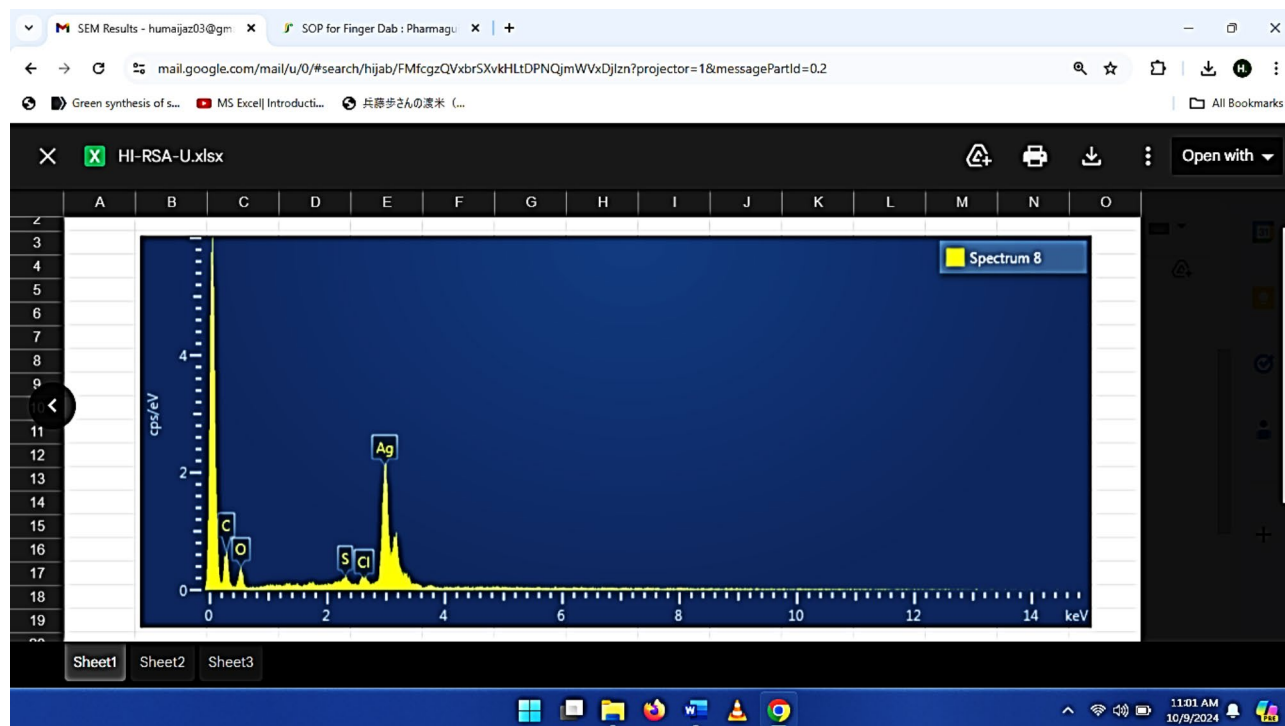


**Fig. 8.** The Ag signals and signals from other elements present in spent black tea.

The peak of malachite green in textile waste spectra showed that the initial absorption signal was plotted at 2.3, while the final absorption signal of the sample exposed to condensing light was found to be 1.6. The efficiency of degradation treatment was further enhanced by the sunlight treatment and the sample exposed to sunlight showed the optical density of 1.3. Thus, malachite green was found to be reduced by 30.43% in condensing light and 43.47% in sunlight. The methylene blue peak fell from the initial OD of 1.2 to 0.9 in condensing light to 0.5 in sunlight. The degradation activity of methylene blue was recorded as 25% in condensing light and 58.3% in sunlight (Fig. 10). The absorption signal of pure malachite green was dropped from the 0.75 to 0.5 and 0.3 for condensing light and sunlight respectively (Fig. 10). The methylene blue standard also exhibited a fall from initial absorption signal of 0.9 to 0.75 in condensing light to 0.55 in the sunlight (Fig. 11). The degradation activity of pure methylene blue was recorded as 16% for condensing light and 35% for sunlight. The pure malachite green exhibited the degradation activity of 33.3% and 60% in sunlight. (Fig. 12). The outcomes of studies on malachite green were resonated with the research of Iqra et al.<sup>34</sup> in which the outcomes were found to be dependent on the sunlight and other catalysts. Similarly, the studies such as Al-Zaban et al.<sup>55</sup>, researched on catalytic degradation of methylene blue by honey mediated AgNPs. The study by Vanaja et al.<sup>57</sup>, confirmed the sunlight catalysed potential of AgNPs for methylene blue degradation. The difference in degradation efficiency between methylene blue and malachite green was due to their distinct chemical structures. The conjugated heterocyclic structure of methylene blue, a thiazine dye with atoms of sulphur and nitrogen, gives it stability through aromatic resonance<sup>58</sup>. Malachite green, on the other hand, is a triphenylmethane dye that is more prone to deterioration due to its weaker central carbon. Because of its less stable structure, malachite green degrades more readily than methylene blue<sup>59</sup>.

The photocatalytic degradation of malachite green (MG) using Ag-NPs under light irradiation is a multi-step process. The process begins with the effective adsorption of MG molecules, followed by the absorption of light photons, which energize the reaction. This energy enhances the molecular vibrations of MG, exposing structural sites that can be attacked by AgNPs. Light irradiation in photocatalysis creates electron-hole pairs ( $e^-/h^+$ ) that aid in oxidation and reduction reactions. The  $h^+$  ions combine with hydroxide ions ( $OH^-$ ) to create hydroxyl radicals ( $\cdot OH$ ), allowing for the oxidative destruction of MG. Photoinduced electrons form more  $\cdot OH$  radicals that aid in degradation<sup>4,5</sup>. AgNPs serve an important function by trapping electrons in the conduction band, reducing electron-hole recombination, and therefore, increasing photocatalytic effectiveness. However, the process's reliance on light also has certain drawbacks, including the requirement for adequate sunlight intensity and the possibility of decreased efficacy in low light or indoor conditions. Furthermore, extended exposure to light may cause the nanoparticles to degrade, which would reduce their long-term catalytic activity. Deeper understanding of the underlying mechanisms and constraints would be possible with additional research into the ideal light conditions and stability of SBT-AgNPs under various light exposures.



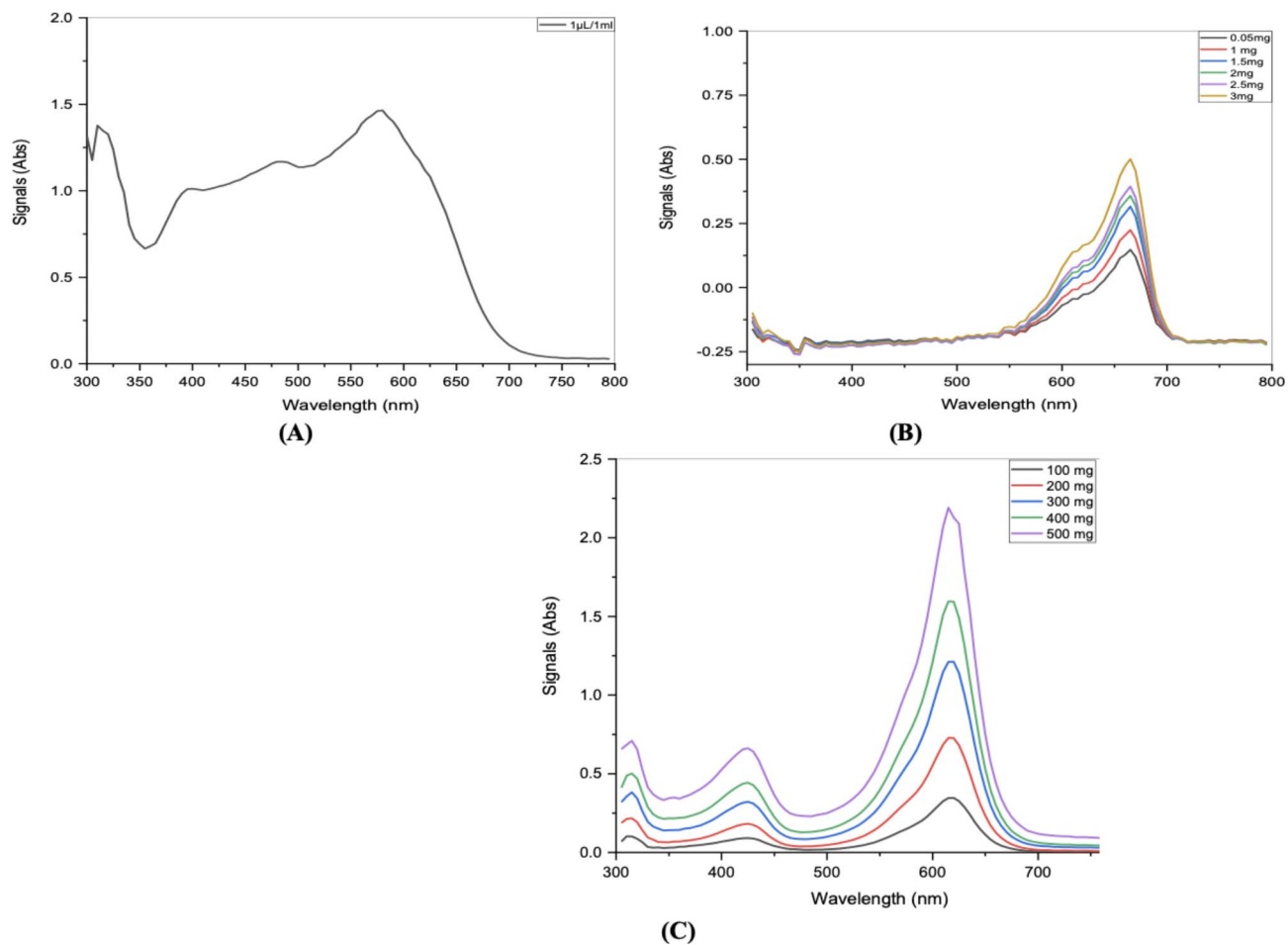


**Fig. 9.** (A) The SPR of textile wastewater (B) the standard preparation of methylene blue at various concentrations (C) the standard preparation of malachite green at various concentrations.

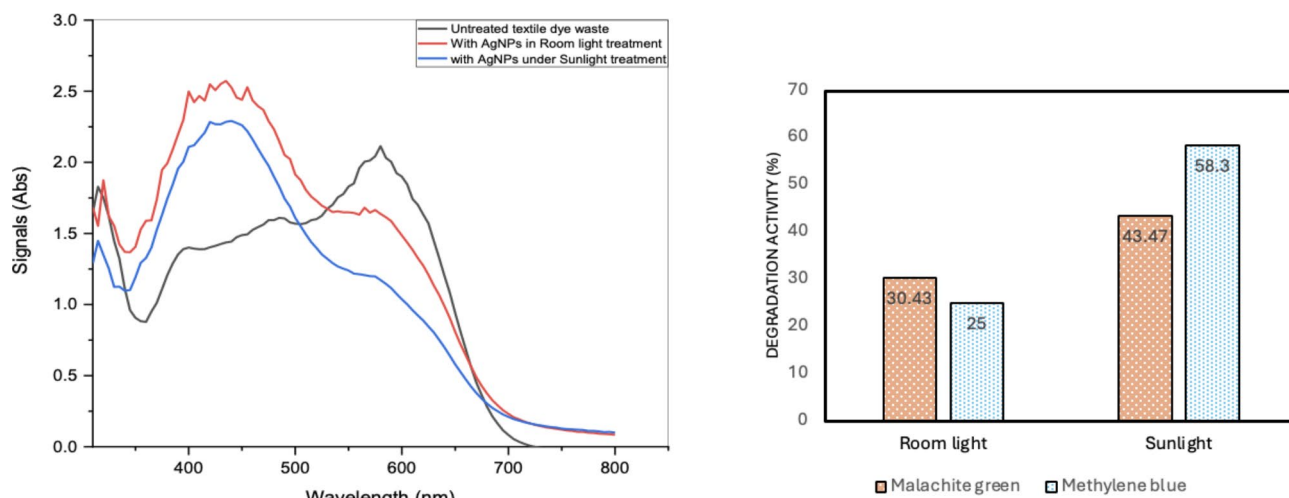


**Fig. 10.** The degradation of textile dyes in wastewater by SBT-AgNPs in the presence of room light and sunlight.

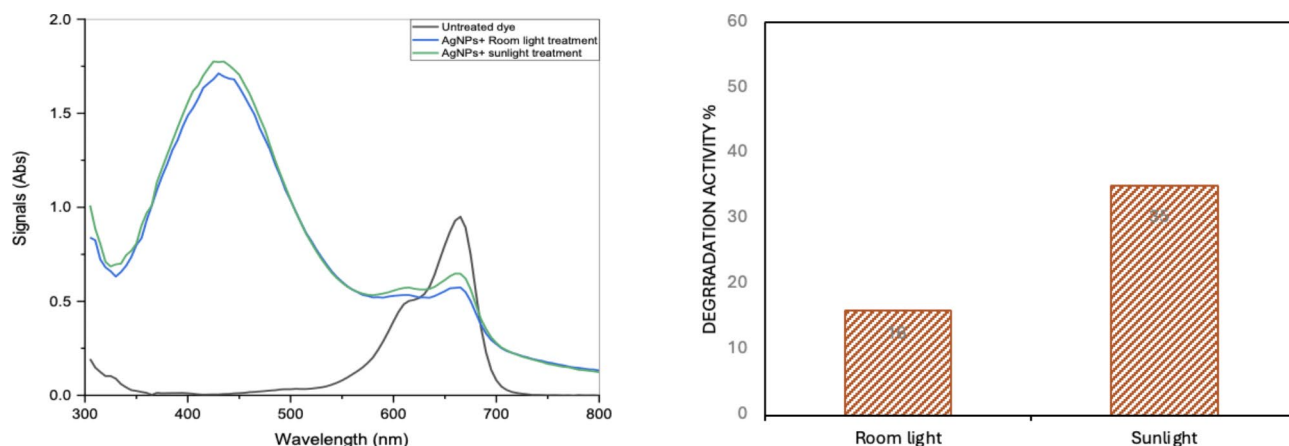


**Fig. 11.** The degradation of pure methylene blue dye by SBT-AgNPs in presence of room light and sunlight.

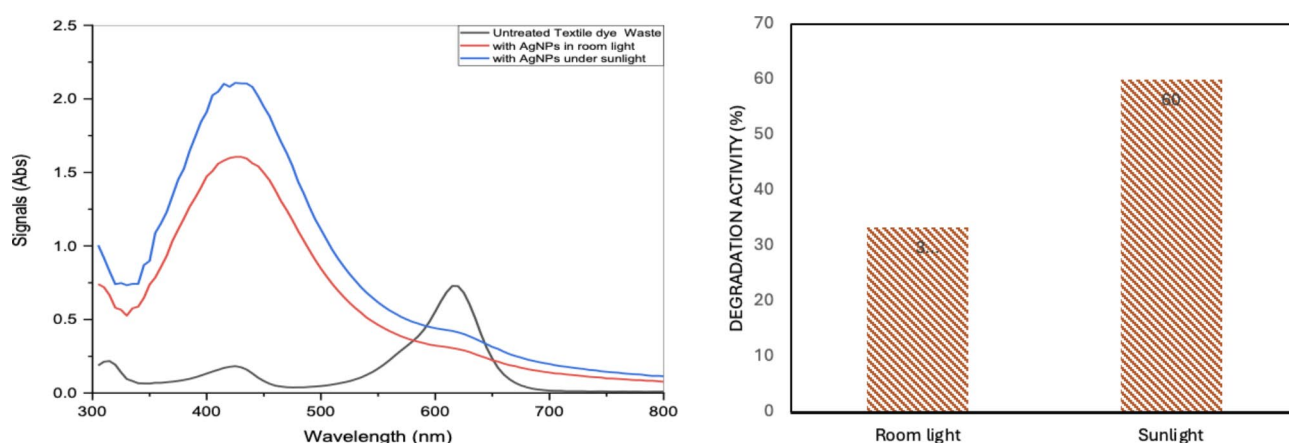


**Fig. 12.** The degradation of pure malachite green dye by SBT-AgNPs in presence of room light and sunlight.

## Conclusion

The study successfully demonstrated the results of optimization studies on the yield of SBT-AgNPs. Different parameters in collaboration enhanced the SBT-AgNPs production. The characterization by XRD, Zeta potential, EDX and SEM. The outcomes exhibited extraordinary improvement in the stability, purity particle sizes and crystallinity as compared to chemically synthesized AgNPs. The SBT-AgNPs also displayed excellent dye removal capabilities up to 58.3 and 43.47% against methylene blue as well as 33.3 and 60% against malachite green in just 180 min of exposure. The achievement of this objective was remarkable considering the complex composition of dyes in wastewater when compared to lab prepared standard solution of methylene blue. In future study expect to further explore the enhanced activity of SBT-AgNPs in the treatment of textile dyes horizontally and vertically. The spent black tea holds great potential as a reducing and capping agent for bioremediation as well as industrial catalyst for degradation reactions.

## Data availability

All the data generated in this research work has been included in this manuscript.

Received: 29 November 2024; Accepted: 7 January 2025

Published online: 13 January 2025

## References

1. Menezes, L. B. et al. Calcium oxide nanoparticles: Biosynthesis, characterization and photocatalytic activity for application in yellow tartrazine dye removal. *J. Photochem. Photobiol. A*. **447**, 115182 (2024).
2. Marimuthu, S. et al. Silver nanoparticles in dye effluent treatment: A review on synthesis, treatment methods, mechanisms, photocatalytic degradation, toxic effects and mitigation of toxicity. *J. Photochem. Photobiol., B*. **205**, 111823 (2020).



3. Rajasekar, R., Thanasamy, R., Samuel, M., Jebakumar Immanuel Edison, T. N. & Raman, N. Eco-friendly green synthesis of silver nanoparticles using *Luffa acutangula*: Synthesis, characterisation and catalytic degradation of methylene blue and malachite green dyes. *Int. J. Environ. Anal. Chem.* **104** (10), 2255–2267 (2024).
4. Tsvetkov, M., Zaharieva, J. & Milanova, M. Ferrites, modified with silver nanoparticles, for photocatalytic degradation of malachite green in aqueous solutions. *Catal. Today*. **357**, 453–459 (2020).
5. Xu, Z. et al. Enhanced photocatalytic degradation of malachite green dye using silver–manganese oxide nanoparticles. *Molecules* **28** (17), 6241 (2023).
6. Lanjwani, M. F., Tuzen, M., Khuhawar, M. Y. & Saleh, T. A. Trends in photocatalytic degradation of organic dye pollutants using nanoparticles: A review. *Inorg. Chem. Commun.* **159**, 111613 (2024).
7. Emerich, D. F. & Thanos, C. G. Nanotechnology and medicine. *Expert Opin. Biol. Ther.* **3** (4), 655–663. <https://doi.org/10.1517/14712598.3.4.655> (2003).
8. Arroyo, G. V. et al. Green synthesis of silver nanoparticles for application in cosmetics. *J. Environ. Sci. Health part. A*. **55** (11), 1304–1320. <https://doi.org/10.1080/10934529.2020.1790953> (2020).
9. Zhang, W. & Jiang, W. Antioxidant and antibacterial chitosan film with tea polyphenols-mediated green synthesis silver nanoparticle via a novel one-pot method. *Int. J. Biol. Macromol.* **155**, 1252–1261. <https://doi.org/10.1016/j.ijbiomac.2019.11.093> (2020).
10. Joseph, S. & Mathew, B. Microwave-assisted green synthesis of silver nanoparticles and the study on catalytic activity in the degradation of dyes. *J. Mol. Liq.* **204**, 184–191 (2015).
11. Bhushan, B. Introduction to nanotechnology. *Springer handbook of nanotechnology*, 1–19. (2017). [https://doi.org/10.1007/978-3-662-54357-3\\_1](https://doi.org/10.1007/978-3-662-54357-3_1)
12. Saleem, A. et al. The characterization and study of antibacterial, free radical scavenging, and anticancer potential of *livistona chinensis*-mediated silver nanoparticles. *Molecules* **28** (23), 7773. <https://doi.org/10.3390/molecules28237773> (2023).
13. Al-Radadi, N. S. & Abu-Dief, A. M. Silver nanoparticles (AgNPs) as a metal nano-therapy: possible mechanisms of antiviral action against COVID-19. *Inorganic and nano-metal chemistry*, 1–19. (2022). <https://doi.org/10.1080/24701556.2022.2068585>
14. Shouket, S. et al. Biosynthetically produced glucose oxidase immobilized silver nanoparticle bioconjugate treatment improves the shelf life of mango fruit: An innovative method towards food safety and sustainability. *Biomass Conv Bioref.* **14**, 31357–31368. <https://doi.org/10.1007/s13399-023-04753-1> (2024).
15. Hussain, Z. et al. Synthesis and characterization of silver nanoparticles mediated by the *Mentha Piperita* leaves Extract and Exploration of its antimicrobial activities. *J. Chil. Chem. Soc.* **68** (2), 5865–5870. <https://doi.org/10.4067/s0717-97072023000205865> (2023).
16. Arshad, F. et al. Bioinspired and green synthesis of silver nanoparticles for medical applications: A green perspective. *Appl. Biochem. Biotechnol.* **196** (6), 3636–3669. <https://doi.org/10.1007/s12010-023-04719-z> (2024).
17. Bhakya, S. et al. Catalytic degradation of organic dyes using synthesized silver nanoparticles: A green approach. *J. Bioremediat. Biodegradation*. **6** (5), 1. <https://doi.org/10.4172/2155-6199.1000312> (2015).
18. Qing, W., Chen, K., Wang, Y., Liu, X. & Lu, M. Green synthesis of silver nanoparticles by waste tea extract and degradation of organic dye in the absence and presence of H<sub>2</sub>O<sub>2</sub>. *Appl. Surf. Sci.* **423**, 1019–1024. <https://doi.org/10.1016/j.apsusc.2017.07.007> (2017).
19. Kumar, J. A. et al. A focus to green synthesis of metal/metal based oxide nanoparticles: various mechanisms and applications towards ecological approach. *J. Clean. Prod.* **324**, 129198. <https://doi.org/10.1016/j.jclepro.2021.129198> (2021).
20. Druzian, D. M. et al. Cerium oxide nanoparticles: Biosynthesis, characterization, antimicrobial, ecotoxicity and photocatalytic activity. *J. Photochem. Photobiol. A*. **442**, 114773 (2023).
21. Saifuddin, N. N., Matussin, S. N., Fariduddin, Q. & Khan, M. M. Potentials of roots, stems, leaves, flowers, fruits, and seeds extract for the synthesis of silver nanoparticles. *Bioprocess and biosystems engineering*, 1–19. (2024). <https://doi.org/10.1007/s00449-024-03044-x>
22. Al-Ogaidi, I. et al. Antibacterial and cytotoxicity of silver nanoparticles synthesized in green and black tea. *World Journal of Experimental Biosciences (ISSN: 2313-3937)*, 39–45. (2017).
23. Chandra, A. et al. Green synthesis of silver nanoparticles using tea leaves from three different elevations. *Chem. Select.* **5** (14), 4239–4246. <https://doi.org/10.1002/slct.201904826> (2020).
24. Alattar, A. M. & Al-tememe, N. A. Preparation and analysis of silver nanoparticles (AgNPs) by plant extract techniques of green tea and study optical and structural properties. *Nano Med. Mater.* <https://doi.org/10.59400/nmm.v3i1.145> (2023).
25. Jing, Y. et al. Structural characterization, antioxidant and antibacterial activities of a novel polysaccharide from *Zingiber officinale* and its application in synthesis of silver nanoparticles. *Front. Nutr.* **9**, 917094. <https://doi.org/10.3389/fnut.2022.917094> (2022).
26. Rolim, W. R. et al. Green tea extract mediated biogenic synthesis of silver nanoparticles: characterization, cytotoxicity evaluation and antibacterial activity. *Appl. Surf. Sci.* **463**, 66–74. <https://doi.org/10.1016/j.apsusc.2018.08.203> (2019).
27. Graf, P. et al. Peptide-coated silver nanoparticles: Synthesis, surface chemistry, and pH-triggered, reversible assembly into particle assemblies. *Chemistry* **15** (23), 5831–5844. <https://doi.org/10.1002/chem.200802329> (2009).
28. Jaast, S. & Grewal, A. Green synthesis of silver nanoparticles, characterization and evaluation of their photocatalytic dye degradation activity. *Curr. Res. Green. Sustainable Chem.* **4**, 100195 (2021).
29. Trieu, Q. A., Le, C. T. B., Pham, C. M. & Bui, T. H. Photocatalytic degradation of methylene blue and antibacterial activity of silver nanoparticles synthesized from *Camellia sinensis* leaf extract. *J. Exp. Nanosci.* **18** (1), 2225759. <https://doi.org/10.1080/17458080.2023.2225759> (2023).
30. Zhu, H., Wang, Y., Liu, Y., Xia, Y. & Tang, T. Analysis of flavonoids in *Portulaca oleracea* L. by UV–vis spectrophotometry with comparative study on different extraction technologies. *Food. Anal. Methods*. **3**, 90–97. <https://doi.org/10.1007/s12161-009-9091-2> (2010).
31. Ahari, H. et al. Synthesis of the silver nanoparticle by chemical reduction method and preparation of nanocomposite based on AgNPs. Proceedings of the 4th world congress on mechanical, chemical, and material engineering, MCM, (2018).
32. Widadalla, H. A. et al. Green synthesis of silver nanoparticles using green tea leaf extract, characterization and evaluation of antimicrobial activity. *Nanoscale Adv.* **4** (3), 911–915. <https://doi.org/10.1039/D1NA00509J> (2022).
33. Yu, Y. H. et al. Electrical, morphological, and electromagnetic interference shielding properties of silver nanowires and nanoparticles conductive composites. *Mater. Chem. Phys.* **136** (2–3), 334–340 (2012).
34. Iqra, Khattak, R. et al. Green synthesis of silver oxide microparticles using green tea leaves extract for an efficient removal of malachite green from water: Synergistic effect of persulfate. *Catalysts* **13** (2), 227. <https://doi.org/10.3390/catal13020227> (2023).
35. Wirwis, A. & Sadowski, Z. Green synthesis of silver nanoparticles: Optimizing Green Tea Leaf extraction for enhanced Physicochemical Properties. *ACS Omega*. **8** (33), 30532–30549. <https://doi.org/10.1021/acsomega.3c03775> (2023).
36. Kharabi Masooleh, A., AhmadiKhah, A. & Saidi, A. Green synthesis of stable silver nanoparticles by the main reduction component of green tea (*Camellia sinensis* L.). *IET Nanobiotechnol.* **13** (2), 183–188. <https://doi.org/10.1049/iet-nbt.2018.5141> (2019).
37. Uddin, M. J., Chaudhuri, B., Pramanik, K., Mridha, T. R. & Chaudhuri, B. Black tea leaf extract derived Ag nanoparticle-PVA composite film: Structural and dielectric properties. *Mater. Sci. Engineering: B*. **177** (20), 1741–1747. <https://doi.org/10.1016/j.mseb.2012.09.001> (2012).
38. Nikam, S. & Chaudhari, S. Optimization of Green Synthesized Black Tea Nanoparticles using Central Composite Design. *Int. J. Pharm. Invest.* **13** (1). <https://doi.org/10.5530/223097131651> (2023).

39. Okafor, F., Janen, A., Kukhtareva, T., Edwards, V. & Curley, M. Green synthesis of silver nanoparticles, their characterization, application and antibacterial activity. *Int. J. Environ. Res. Public Health*. **10** (10), 5221–5238. <https://doi.org/10.3390/ijerph10105221> (2013).
40. Hermanto, D. et al. Bio-mediated electrochemically synthesis of silver nanoparticles using green tea (*Camellia sinensis*) leaves extract and their antibacterial activity. *S. Afr. J. Chem. Eng.* **47** (1), 136–141. <https://doi.org/10.1016/j.jallcom.2022.164300> (2024).
41. Sun, Q. et al. Green synthesis of silver nanoparticles using tea leaf extract and evaluation of their stability and antibacterial activity. *Colloids Surf., a*. **444**, 226–231. <https://doi.org/10.1016/j.colsurfa.2013.12.065> (2014).
42. AL-Hashimi, M. M. S. Production of silver nanoparticles using spent coffee ground for antibacterial effect. *Doctoral dissertation, Universiti Teknologi Malaysia*. (2021). <https://eprints.utm.my/101648/1/MaryamMubarakSaidMFS2021.pdf>
43. Verma, A. & Mehata, M. S. Controllable synthesis of silver nanoparticles using neem leaves and their antimicrobial activity. *J. Radiation Res. Appl. Sci.* **9** (1), 109–115. <https://doi.org/10.1016/j.jrras.2015.11.001> (2016).
44. Salayová, A. et al. Green Synthesis of Silver Nanoparticles with antibacterial activity using various Medicinal Plant extracts: morphology and Antibacterial Efficacy. *Nanomaterials* **14** (4), 1005. <https://doi.org/10.3390/nano11041005> (2021).
45. Ali, M. H. et al. Analysis of crystallographic structures and properties of silver nanoparticles synthesized using PKL extract and nanoscale characterization techniques. *ACS Omega*. **8** (31), 28133–28142. <https://doi.org/10.1021/acsomega.3c01261> (2023).
46. Manikandan, E. & Krishnan, V. Green synthesis of silver nanoparticles using *Piper nigrum* concoction and its anticancer activity against MCF-7 and Hep-2 cell lines. *J. Antimicrob. Agent.* **2**, 3–7 (2016).
47. Li, S. et al. Green synthesis of silver nanoparticles using Capsicum annuum L. extract [10.1039/B615357G]. *Green Chem.* **9** (8), 852–858. <https://doi.org/10.1016/j.jddst.2023.104165> (2007).
48. Ninsiima, H. I. et al. Green tea silver nanoparticles improve physiological motor and cognitive function in BALB/c mice during inflammation. *Heliyon*, **9**(3). (2023).
49. Shyamalgowri, S. et al. In vitro anticancer activity of silver nanoparticles phyto-fabricated by *Hylocereus undatus* peel extracts on human liver carcinoma (HepG2) cell lines. *Process. Biochem.* **116**, 17–25 (2022).
50. Parvathalu, K. et al. Facile synthesis of silver nanoparticles using Green Tea Leaf Extract and Evolution of Antibacterial Activity. *Plasmonics* **18**, 1837–1845. <https://doi.org/10.1007/s11468-023-01899-6> (2023).
51. Goyal, D., Kaur, G., Tewari, R. & Kumar, R. Correlation of edge truncation with antibacterial activity of plate-like anisotropic silver nanoparticles. *Environ. Sci. Pollut. Res.* **24**, 20429–20437. <https://doi.org/10.1007/s11356-017-9630-0> (2017).
52. Giri, A. K. et al. Green synthesis and characterization of silver nanoparticles using *Eugenia Roxburghii* DC. Extract and activity against biofilm-producing bacteria. *Sci. Rep.* **12**, 8383. <https://doi.org/10.1038/s41598-022-12484-y> (2022).
53. Gita, S., Hussan, A. & Choudhury, T. Impact of textile dyes waste on aquatic environments and its treatment. *Environ. Ecol.* **35** (3 C), 2349–2353 (2017).
54. Jain, P., Soni, A., Jain, P. & Bhawsar, J. Phytochemical analysis of *Mentha spicata* plant extract using UV-VIS, FTIR and GC/MS technique. *J. Chem. Pharmacol. Res.* **8** (2), 1–6. <https://doi.org/10.1016/j.crgsc.2021.100195> (2016).
55. Al-Zaban, M. I., Mahmoud, M. A. & AlHarbi, M. A. Catalytic degradation of methylene blue using silver nanoparticles synthesized by honey. *Saudi J. Biol. Sci.* **28** (3), 2007–2013. <https://doi.org/10.1016/j.sjbs.2021.01.003> (2021).
56. Kang, C. W. & Kolya, H. Green synthesis of Ag-Au bimetallic nanocomposites using waste tea leaves extract for degradation Congo red and 4-Nitrophenol. *Sustainability* **13** (6), 3318. <https://doi.org/10.3390/su13063318> (2021).
57. Vanaja, M. et al. Degradation of methylene blue using biologically synthesized silver nanoparticles. *Bioinorg. Chem. Appl.* **2014** (1), 742346. <https://doi.org/10.1155/2014/742346> (2014).
58. Oladoye, P. O., Ajiboye, T. O., Omotola, E. O. & Oyewola, O. J. Methylene blue dye: toxicity and potential elimination technology from wastewater. *Results Eng.* **16**, 100678 (2022).
59. Moumeni, O., Hamdaoui, O. & Pétier, C. Sonochemical degradation of malachite green in water. *Chem. Eng. Process.* **62**, 47–53 (2012).

## Acknowledgements

We express our gratitude to the Vice Chancellor for supplying the required resources. We also acknowledge the research grant with reference no. 667/ORIC/22 provided by ORIC, GCU, Lahore. The authors extend their gratitude to Princess Nourah bint Abdulrahman University Researchers Supporting Project number (PNUR-SP2025R31), Princess Nourah bint Abdulrahman University, Riyadh, Saudi Arabia. The authors also thank the Deanship of Scientific Research (DSR) at King Faisal University under the Project number [KFU250047].

## Author contributions

Conceptualization, Huma Ijaz and Sikander Ali.; Methodology: Rukhma.; Validation, Muhammad Usman Ahmad; Formal analysis, Abid Sarwar.; Investigation, Najeeb Ullah.; Resources, Muhammad Jalal Khan.; Data curation, Ashwag Shami.; Writing—original draft preparation, Fahad Al-Asmari; writing—review and editing, Tariq Aziz; visualization, Abdullah F Alasmari.; supervision, Sikander Ali and Tariq Aziz.; Project administration, Sikander Ali.; Funding acquisition, Tariq Aziz.

## Declarations

## Competing interests

The authors declare no competing interests.

## Additional information

**Correspondence** and requests for materials should be addressed to S.A. or T.A.

**Reprints and permissions information** is available at [www.nature.com/reprints](http://www.nature.com/reprints).

**Publisher's note** Springer Nature remains neutral with regard to jurisdictional claims in published maps and institutional affiliations.

**Open Access** This article is licensed under a Creative Commons Attribution-NonCommercial-NoDerivatives 4.0 International License, which permits any non-commercial use, sharing, distribution and reproduction in any medium or format, as long as you give appropriate credit to the original author(s) and the source, provide a link to the Creative Commons licence, and indicate if you modified the licensed material. You do not have permission under this licence to share adapted material derived from this article or parts of it. The images or other third party material in this article are included in the article's Creative Commons licence, unless indicated otherwise in a credit line to the material. If material is not included in the article's Creative Commons licence and your intended use is not permitted by statutory regulation or exceeds the permitted use, you will need to obtain permission directly from the copyright holder. To view a copy of this licence, visit <http://creativecommons.org/licenses/by-nc-nd/4.0/>.

© The Author(s) 2025